Synthesis and precipitation of silica and titania nano-structures on cellulose fibers by biomineralization processes

Verónica Bouça

May, 2016

Abstract

The goal of this thesis was to develop hybrid materials of cellulose/silica and cellulose/titanium dioxide by exploring the biomineralization ability of the peptide R5 (SSKKSGSYSGSKGSKRRIL). As a first step, the R5-induced precipitation of silica and titanium dioxide nanoparticles in solution was studied. Under the conditions studied (1.5 mM R5, 91 mM precursor, pH 7), the specific activity of R5 for silica and titanium dioxide precipitation was 8.6 ± 2.2 nmol Si/min.nmol R5 and e 6.0 ± 1.0 nmol Ti/min.nmol R5, respectively. SEM analysis showed that precipitates were composed of close to spherical nanoparticles with two individual sizes in the order of 37 and 538 nm for silica; for the titania case, they were in the order of 479 nm. Experiments conducted with a fusion of R5 with a carbohydrate binding module (CBM3) confirmed that R5 maintained its ability to precipitate silica and titanium dioxide, yielding nanoparticles with comparable morphology/size. The ability of R5 and CBM3-R5 to precipitate silica and titanium dioxide in situ paper fibers investigated. When used an amount of 3000 pmol/0.13 cm2, both pre-immobilized R5 (via physical adsorption) and CBM3-R5 (by affinity interactions) were able to precipitate silica, yielding densely packed networks of fused and clustered particles over the cellulose fibers and fibrils in paper. Individual particles obtained with R5 and CBM3-R5 had an average size of around 213 ± 78 nm and 231 ± 39 nm, respectively.

Keywords: Nanoparticles, silica, titanium dioxide, CBM3-R5 protein, paper

Introduction

In the biological sciences, nanoparticles are defined as particles with a size smaller than 1000 nm. Their size is the key feature that allows them to preserve their unique physicochemical properties when compared to bulk materials (Buzea et al., 2007; Li et al., 2011).

Nanoparticles can be divided into two groups: organic and inorganic (Prathna et al., 2010). Organic nanoparticles can be made of a variety of materials such as carbon (fullerenes and nanotubes), polymers (alginate, chitosan) and lipids (like soybean lecithin and stearic acid). Inorganic nanoparticles include several varieties of particles such as magnetic nanoparticles, noble-metal nanoparticles (e.g. gold and silver), semiconductors (e.g. titanium dioxide and zinc oxide) and non-metal nanoparticles (e.g. silica and quantum dots) (Prathna et al., 2010; Grillo et al., 2015). The silica nanoparticles (SiNPs) are being use in several applications such as in biomedical field (e.g. drug delivery, cell markers), and in different industries (e.g. insulators, electronic devices) due to characteristics such as biocompatibility, monodispersity, stability, high drug loading efficiency and their potential for hybridization with other materials, among others (Gholami et al., 2013; Tamba et al., 2015). Titanium dioxide nanoparticles (TiNPs) has been used as an additive agent in food and it works as a coloring agent that promotes opacity and blankness opacity in inks, as well as in personal care products(Li et al., 2014). Furthermore, TiNPs have been commonly applied in sunscreens due to their optical properties, since they have a remarkable ultra violet (UV) absorbance, especially in UV range (Smijs and Pavel, 2011; Li et al., 2014).

The methods used for the synthesis of SiNPs and TiNPs generally require extreme values of pH, temperatures and pressures (Sewell and Wright, 2006; Otzen, 2012). The diatom algae have an external cell wall known as frustules, which exhibit intricate patterns made of amorphous silica in the nano- to micro-meter ranges (Parkinson and Gordon, 1999; Sumper and Kröger, 2004). The biosilicification process of diatom algae offers an alternative to produce nanomaterials under mild reaction conditions, which has inspired researchers for the biomimetic production of inorganic nanomaterials (Kröger et al., 2001). Diatom biosilica, an organic-inorganic hybrid is formed by biomolecules that are firmly attached within amorphous hydrated silica (Sumper and Kröger, 2004). Some of these organic constituents of biosilica have been showed to mediate and accelerate the synthesis of silica nanospheres *in vitro*, using a silicic acid solution under ambient conditions

and neutral pH. These organic components are polycationic polypeptides known as silaffins and long-chain polyamines (Kröger et al., 1999, 2000).

The C-terminal part of poplypetide sil1p of diatom *Cylindrotheca fusiformis* (composed by repeat units R1 to R7) encoded by the silaffin gene, sil1, is subjected to a proteolytic process *in vivo*, generating the silaffin isomorfs of silaffin-1A (silaffin-$1A_1$, silaffin-$1A_2$) and silaffin-1B. The silaffin-$1A_1$ peptides are derived from repeat units R3 to R7 of sil1p. The mature native silaffin-$1A_1$ does not contain the C-terminal tetrapeptides RRIL, which are apparently removed during maturation of sil1p precursor poplypeptide. Moreover, this peptide has post-translations modifications, that consist in lysine residues polyamine-modified, which result in: ε-N,N-dimethyllysine, phosphorylatede ε-N,N,N-trimethyl-δ-hydroxylysine and derivatives of polypropylenimine. Besides these modifications, the native silaffin-$1A_1$ has all of the serine residues phosphorylated (Kröger et al., 2001, 2002; Sumper and Kröger, 2004)

The 19-amino acid-long synthetic R5 (SSKKSGSYSGSKGSKRRIL) is a biomimetic analog of the repeat unit R5 of the C-terminal part of polypeptide silp1 of diatom *Cylindrotheca fusiformis*, which lacks post-translational modifications at its lysine residues (Kröger et al., 1999). The R5 peptide can induce silica precipitation from silicic acid solution, only above pH 6, in contrast with silaffin $1A_1$ that is active in acidic and neutral pH with maximal activity at pH values around 5 (Kröger et al., 1999). Have been suggested that self-assemble of R5 peptide as well as of native silaffins work as template for silicic acid polycondensation (Lechner and Becker, 2015). The RRIL motif are suggest to play a crucial role in the self-assemble mechanism of R5 (Knecht and Wright, 2003; Lechner and Becker, 2014). Have been proposed that the self-assembly of the R5 occurs via the salt bridges formed between the positively charged guanidine groups from arginine (RR) and the negatively charged phosphate anions from the buffer (Lechner and Becker, 2014). Whereas, the self-assembly of native silaffins is also due electrostatic interactions driven by their oppositely charged posttranslational modifications (polyamine moieties and phosphate groups) (Kröger et al., 1999, 2002). Have been confirmed that the lysine residues found in the unmodified R5 are crucial for its silica precipitation activity, due the presence of the positively charged ε-amino groups of the lysine residues, that mediated the silica polycondensation. Furthermore, the number and the position of lysine residues in the sequence of the R5, the chemical nature of neighboring amino acids and their charge showed to influence the silica material morphology (Lechner and Becker, 2014). The ability of the R5 to form amorphous TiNPs has also been studied from a non-natural precursor of titanium (IV) bis(ammonio lactate)dihydroxide (Ti-BALDH, $[CH_3CH(O-)CO_2NH_4]_2Ti(OH)_2$) at ambient conditions (Cole et al., 2006; Sewell and Wright, 2006). The RRIL motif is also required for the self-assembled peptide structure as well as for silica precipitation. However, the R5 peptide can induce titanium dioxide precipitation at absence of phosphate ions, in contrast with the mechanism of silica precipitation wherein the peptide required phosphate ions. (Sewell and Wright, 2006). The R5 peptide have been used for different purposes, such as to encapsulate proteins inside SiNPs by using DNA technology in order to fuse R5 with a desired protein of interest, which is a promising encapsulation method for industrial biocatalysis field (Emond et al., 2012) and biosensing field (Choi et al., 2011).

Composite materials are a combination of two or more chemically different materials that developed a continuous phase, such as polymer with a dispersed phase, namely silica, carbon particles (Raman et al., 2012). These materials have unique properties, different from the ones of their original components taken separately (Raman et al., 2012). Over the last decade, the development of organic-inorganic hybrid materials has become an interesting subject due to the interesting physicochemical properties that turn them into effective materials for an extensive range of applications (Raman et al., 2012). Silica/cellulose hybrid composites and titanium dioxide/cellulose hybrid composites have been created in order to allow taking advantage of the combined properties of the two materials in a single system (Taha et al., 2012; Abdullahil et al., 2015).

The carbohydrate-binding modules plays an important role in the enhancement of the glycoside hydrolases activity by promoting their binding to the carbohydrate substrate (e.g.cellulose) and increasing the concentration of enzymes on the surface substrate (Blake et al., 2006; Arfi et al., 2014). The DNA fusion technology have been used in order to recombine CBMs with other proteins and antibodies for different purposes (Oliveira et al., 2015). Family-3a CBM (CBM3a) from the scaffoldin cellulosome-integrating protein A, plays a crucial role by allowing the whole cellulosome enzyme complex to bind to the cellulosic substrate *Clostridium thermocellum* CipA (Yaniv et al., 2014). Due to the high affinity to cellulose, CBM3a have been used in order to create bioactive paper for immobilization of biomolecules (Rosa et al., 2014).

Materials and Experimental Methods

Reagents

Ammonium molybdate tetrahydrate, oxalic acid dehydrate, metol, 4,5-dihydroxy-1,3-benzenedisulfonic acid disodium salt monohydrate (Tiron), titanium(IV) bis(ammonium lactate) dihydroxide (50 wt % in water) (Ti-BALDH) and tetramethyl orthosilicate (≥99%) (TMOS) were purchased from Sigma-Aldrich. Sodium sulphite anhydrous was purchased from Acros Organics. Sulphuric acid (<95%), HCl (~37%), acetic acid glacial were purchased from Fischer Chemical. Sodium acetate 3. hydratate, sodium phosphate monobasic, sodium phosphate dibasic were purchased from Panreac.

The 19-mer R5 peptide (SSKKSGSYSGSKGSKRRIL, 2013.30 g/mol) was synthesized by GeneCust and its purification was confirmed via HPLC-MS as ≥95%.

Production and purification of recombinant protein CBM3-R5

The CBM3-R5 gene was synthesized and inserted into a pHTP1 expression vector by Nzytech- Genes & Enzymes. A histidine tag was included at the N terminal for purification purposes. The final vector has 5973 bp with kanamycin resistance.

MGSSHHHHHHSSGPQQGLRPVSGNLKVEFYNSNPSDTTNSINPQFKVTNTGSSAIDLSKLTLRYYYTVDGQ
KDQTFWCDHAAIIGSNGSYNGITSNVKGTFVKMSSSTNNADTYLEISFTGGTLEPGAHVQIQGRFAKNDWS
NYTQSNDYSFKSASQFVEWDQVTAYLNGVLVWGKEPGGSSKKSGSYSGSKGSKRRIL

Figure 1. Amino acid sequence of CBM3-R5 with 199 residues. CBM3, R5 and his tag.

After the transformation of *E. coli* BL21(DE3), cells were grown in LB broth supplemented with 30 µg/mL kanamycin and were incubated overnight at 37 ºC in an orbital shaker at 250 rpm. Expression was induced at an OD600 nm of 0.5 with 1 mM isopropyl β- D-1-thiogalactopyranoside (IPTG). Cells were harvested 12 h after induction by (4 000 g, 4ºC,10 minutes), re-suspended in a minimum volume 50 mM sodium phosphate buffer at pH 7, and disrupted by sonication pulse mode (BANDELIN ultrasonic homogenizer SONOPULS HD 3200, type MS 72) with 30 W at 6 minutes, cycles of 30 seconds. Cell debris were removed by centrifugation at 9000 g for 20 min at 4ºC and the resulting supernatant containing the fusion protein was filtered using a 0.22 µm syringe filter prior to chromatography. Then, purification of the CBM-R5 was performed by Ni-affinity chromatography using a HisTrap FF column of 1 mL from in a Äkta 10 Purifier system (GE Healthcare). The column was equilibrated with 5 column volumes of buffer (10 mM imidazole, 50 mM NaHEPES, 1 M NaCl, 5 mM $CaCl_2$) and loaded with 2 mL of filtered supernatant. The column was washed with 20 column volume of the equilibration buffer and then with 20 column volumes of a similar buffer containing 35 mM imidazole. The CBM3-R5 was eluted with 20 column volumes of a buffer containing 300 mM imidazole. The CBM3-R5 purity was evaluated by sodium dodecyl sulfate polyacrylamide gel electrophoresis (SDS-PAGE) in a 12% acrylamide gel stained with Coomassie Brilliant Blue and the concentration of purified CBM3-R5 was determined by using the Pierce™ BCA (Bicinchoninic Acid) Protein Assay Kit according to the protocol from Thermo scientific – Microplate procedure (Thermo Fischer scientific Inc., 2002). The purified CBM3-R5 was stored at -20º C until required.

Silica precipitation assay

The *in vitro* silica precipitation was based on the method described by Kröger et al. (Kröger et al., 1999). A 1 M silicic acid solution was freshly prepared by dissolving TMOS in 1 mM aqueous HCl during 4 minutes before each assay. R5 was dissolved in 50 mM sodium phosphate buffer at pH 7 to a final concentration of 1.65 mM and final volume of 10 µL in a PCR tube. Then, 1 µL of silicic acid solution was added and the mixture was incubated at room temperature for 5 minutes. The reaction stopped by placing the tubes on ice and silica precipitates were separated by centrifugation at 14 000 g on a Hermle Z233 M-2 High Speed Microcentrifuge for 5 minutes. The supernatant was removed by pipetting and the silica-containing pellet was washed twice with milli-Q water and centrifuged as before. The obtained pellet was dried under vacuum overnight.

Titanium dioxide precipitation assay

In vitro precipitation of titanium dioxide was performed as described for silica. The R5 peptide was dissolved in 50 mM sodium phosphate buffer at pH 7 to a final concentration of 1.65 mM and final volume of 10 µL in a PCR tube. Then, 1 µL of 1 M aqueous solution of Ti-BALDH was added and the mixture was incubated at room temperature for 5 minutes. The reaction was stopped by placing the tubes on ice and titanium dioxide precipitates were separated by centrifugation at 14 000 g on a Hermle Z233 M-2 High Speed Microcentrifuge for 5 minutes. The supernatant was removed by pipetting and the titanium dioxide-containing

pellet was washed twice with water milli-Q and centrifuged as before. Finally, the obtained pellet was dried under vacuum overnight

The blue silicomolybdic assay

The collected dried pellets obtained from precipitation reactions were mixed with 10 µl of 1 M of sodium hydroxide at 95 ºC during 30 minutes performed by using Labnet AccuBlock™ Digital Dry Bath (block chamber D1102) in order to solubilize silica back into silicic acid.

The blue silicomoybdic assay was used for quantification of silicon (Coradin et al., 2004; Nelson and Arrington, 2010). The blue silicomolybdic assay was adapted to 96-well polystyrene microplates (Greiner Bio-one). Each well was loaded with 65 µL of the acidified ammonium molybdate solution (8 g/L) and with 162 µL of sample/working standards (triplicates). After 10 minutes, a freshly prepared solution of metol-sulfite reagent, 10% oxalic acid, 50% acid sulfuric, water milli-Q (3:1:1:3.8) was prepared and 98 µL were added to each well. The blue color was left to develop over 2 hours at room temperature, before measuring the absorbance at a wavelength of 810 nm in a spectrophotometer SpectraMax Plus 384 Microplate. The amount of silicon was calculated from a calibration curve conducted with 1 mM silicic acid generated by TMOS standard solution. All measurements were repeated at least in triplicate.

Titanium supernatant quantification by spectrophotometric assay with tiron

Titanium was determined using Tiron (4,5-dihydroxy-1,3-benzene disulfonic acid), a reagent that reacts with titanium to form a soluble yellow Ti-Tiron complex which can be measured at 380 nm (Moharir, A.V., Sarma, K.A., Murti Krishna, 1972; Cole et al., 2006).

The Tiron spectrophotometric assay was performed in a 96-well polystyrene microplate. Each well was loaded with 20 µL of the 4% Tiron solution and with 180 ul of sample/working standards in 1.5 M sodium acetate buffer (pH 5.3). The yellow color was left to develop over 1 hour at room temperature, before measuring the absorbance at a wavelength of 380 nm in a spectrophotometer SpectraMax Plus 384 Microplate.

The amount of titanium was calculated from a calibration curve conducted with 1 mM Ti-BALDH standard solution.

Scanning Electron Microscopy

Scanning electron microscopy (SEM) was used to analyze the morphology and evaluate the size of the synthesized particles of silica and titanium dioxide. The precipitated material was washed, collected and then suspended in milli-Q water. A drop was added to a SEM support and left to dry. The sample was then coated with gold-palladium and analyzed with a scanning electron microscopy JSM – 7001F from JEOL. The obtained SEM micrographs were analyzed by a public domain image processing software ImageJ (National Institutes of Health) in order to measure the diameter of the particles.

Silica and titanium dioxide precipitation on the paper

Whatman no. 1 chromatography paper (catalog number: 3001-878) was used in all the assays. The wax printing method (Xerox ColorQube 8570 color printer) was used to pattern arrays of 4 mm diameter circumferences (refereed as spot). After printing, the paper was heated to 150 ºC on a heat plate for 2 min in order to melt the wax and allow it to diffuse vertically across the paper section. Thus, circular reaction areas confined by a uniform hydrophobic barrier were created being able to contain aqueous liquids within. Silica and titanium dioxide precipitation was performed in the same way. The concentration of the TMOS and Ti-BALDH precursors (91 mM) as also the reaction time (5 minutes) were the same used in the solution reaction precipitation. Three different concentrations of recombinant CBM-R5 and R5 peptide were tested in order to evaluate the density and distribution of the precipitated material. Briefly, 1 µl of buffer containing 3 000 pmol, 30 pmol or 3 pmol of R5 or CBM3-R5 were added to each spot and allowed to dry for 30 minutes at room temperature. Each circular reaction area was then individualized by cutting paper into 1 cm x 1 cm squares. Precipitation reactions were then performed in 2 mL micro centrifuge tubes by immersing each square piece of paper in 1 mL of a 91 mM precursor solution in sodium phosphate buffer at pH 7 for 5 minutes at room temperature. Protein-free controls were prepared by immersing paper pieces in the precursor solution. After 5 minutes of incubation, samples were taken from the solutions and let to dry at room temperature. In the case of the silica, the silicic acid solution 1 M was freshly prepared by dissolving TMOS in 1 mM aqueous HCL during 8 minutes before each assay and then was prepared 91 mM of silicic acid solution.

Results and discussion

Precipitation of silica induced by the R5 peptide

A first set of experiments was set up to check the impact of R5 on silica precipitation. In these experiments, silicic acid solutions in phosphate buffer at pH 7 were added either to phosphate buffer or to phosphate buffer with 1.5 mM of R5. While no precipitation was observed in the absence of the peptide, a white turbidity rapidly developed in about 30 seconds when the silicic acid was contacted with the peptide solution. This result confirmed that R5 is required to promote silica precipitation.

Furthermore, indirect quantification of the silicon on the precipitates was achieved by digesting silica pellets with NaOH and determining the dissolved silica (essentially monosilicic acid, $Si(OH)_4$) using the silicomolybdic acid spectrophotometric method (Kröger et al., 1999; Coradin et al., 2004). For the experimental conditions used in this work (11 µL, 91 mM silicic acid, 1.5 mM (16.5 nmol) R5, phosphate buffer pH 7), the amount of silicon precipitated after 5 minutes was 713.1 ± 182.4 nmol. Thus, the specific silica precipitation activity obtained here was 8.6 ± 2.2 nmol Si/min.nmol R5, which is of the order of magnitude of the specific activity of 3.59 ± 0.16 nmol of Si/min.nmol R5 obtained with 2 mM of R5 by Knecht and Wright (Knecht and Wright, 2003)

SEM was used to observe the morphology of the particles of R5-precipitated silica. The SEM micrographs in Figure 2 shows that the silica precipitated by R5 is characterized by a heterogeneous size distribution. In terms of size, two main populations of spherical SiNPs are clearly observed in Figure 2A. The population with larger size is characterized by particles with diameters around 538 ± 76 nm, whereas the population with smaller sizes, which seems to predominate, is characterized by diameters of the order of 37 ± 6 nm. Fusion between two or more spherical particles can also be observed, especially for the case of the larger particles (see fused particles circled in orange in Figure 2A). This size discrepancy does not seem to be characteristic of this peptide. According to previous reports, Nam et al obtained SiNPs with sizes in the range of 600 to 700 nm (Nam et al., 2009), Knecht and Wright reported SiNPs with a range of 250 to 450 (Knecht and Wright, 2003), Senior et al and Naik et al obtained SiNPs with a size of about 500 nm (Naik et al., 2003; Senior et al., 2015).

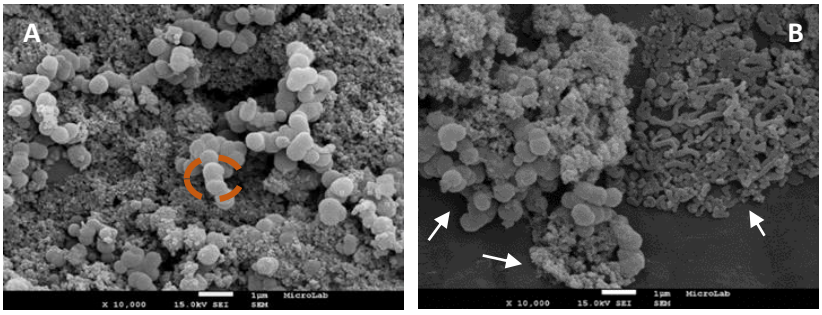

Figure 2. SEM micrographs of SiNPs induced by R5. The A, B a scale bar of 1 µm. A and B have micrographs at magnification of x 10,000. Arrows indicate three different main populations of morphologies/size of SiNPs. The circles indicate what seems to be a fusion between two particles (orange circle).

In addition to the spherical morphology of SiNPS, clusters of elongated forms of silica with different lengths were also observed, some of which were rolled up on themselves (Figure 1B). This morphology was not expected because the R5 peptide have been reported to produce spherical morphology particles under static conditions (Naik et al., 2003).

Titanium dioxide precipitation induced by R5

As in the case of silica, R5 is also required to promote amorphous titanium dioxide precipitation from the precursor Ti-BALDH under ambient conditions. The conditions of the precipitation were the same for silica precipitation. The peptide induced almost instantly the titanium dioxide precipitation, originating a large turbidity. No titanium dioxide precipitation was observed in the absence of the peptide at room temperature.

The titanium left in the supernatant after precipitation halted was further quantified by the Tiron complexation assay and used to estimate the amount of precipitated titanium by mass balance. The amount of precipitated titanium after 5 minutes was 492.0 ± 85.0 nmol with the same conditions used for silica precipitation (11 µL, 91 mM titanium, 1.5 mM (16.5 nmol) R5, phosphate buffer pH 7). The specific activity of R5 for titanium precipitation was of 6.0 ± 1.0 nmol of Ti/min.nmol R5. This result is of the order the same magnitude obtained in previous reports, for example, Sewell and Wright obtained a specific activity of 2.16 ± 0.23 nmol Ti/min.nmol R5 (Sewell and Wright, 2006).

In order to evaluate the morphology as well as the size of the particles induced by 1.5 mM R5 and 91 mM titanium precursor for 5 minutes, SEM analysis were made (Figure 3).

The SEM micrographs (Figure 3) of the spherical TiNPs showed a diameter of about 479 ± 92 nmol. In the figure 3 A, is possible to observe TiNPs clusters, where the particles are fused between them. Moreover, the surface particles seem to be rough (Figure 3, B). There are structures that appeared to be a result of the consecutive fusion between the particles, which do not allow to distinguish spherical single particles (circle blue). According to the previous works, different sizes of titanium dioxide particles were obtained, such as 50 ± 20 nm (Sewell and Wright, 2006) and 3.2 ± 1.5 µm (Cole et al., 2006).

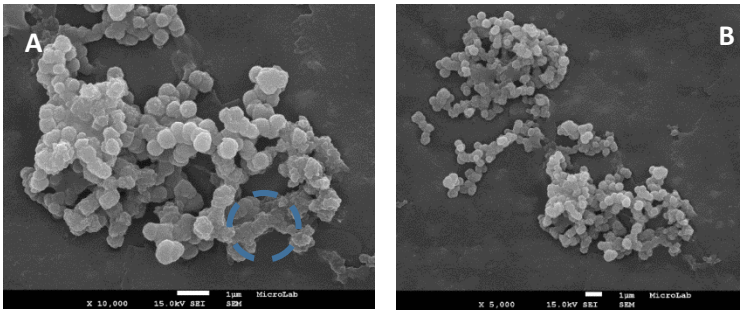

Figure 3. SEM micrographs of TiNPs induced by R5. Scale bar of 1 µm. A and B micrographs have magnifications of x 10, 000 and x 5, 000, respectively.

Precipitation of silica and titanium dioxide induced by CBM3-R5

A CBM3-R5 fusion was designed, produced and purified with the goal of immobilizing the R5 peptide in cellulose matrices and attempt to precipitate silica and titanium dioxide *in situ*. An initial set of experiments was performed to investigate the ability of the CBM3-R5 fusion to promote precipitation in solution. The results showed that the silica precipitation activity of R5 was not affected by its fusion with CBM3. The morphology of the precipitate obtained with 1.5 mM CBM3-R5 and 91 mM of TMOS at pH 7 in the 50 mM phosphate buffer was observed through SEM analysis and compared with the morphology of SiNPs obtained only with R5**.**

As can be observed, the fusion protein induces the formation of partially homogenous spherical silica particles with sizes around 819.69 ± 178.38 nm, larger than the particles obtained with R5 (Figure 4).

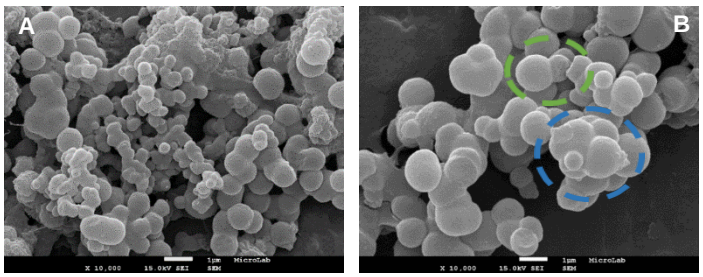

Figure 4. SEM micrographs of SiNPs induced by CBM3-R5 in 50 mM phosphate buffer at pH 7. Micrographs were obtained with magnifications of x 10, 000 (A, B). Scale bar 1 µm.

The CBM3-R5 protein was also able to induce titanium dioxide precipitation in solution (Figure 5). As with the silica particles, aggregated spherical particles of titanium dioxide with sizes around 528 ±77 were observed (Figure 5).

In similar, with SiNPs obtained with this protein, it was observed clusters of the TiNPs, where the TiNPs were hardly connected to each other (Figure 5, A). In addition to partially spherical morphology, elongated structures were observed, which seem to result from the fusion between the TiNPs (Figure 5B, blue circle).

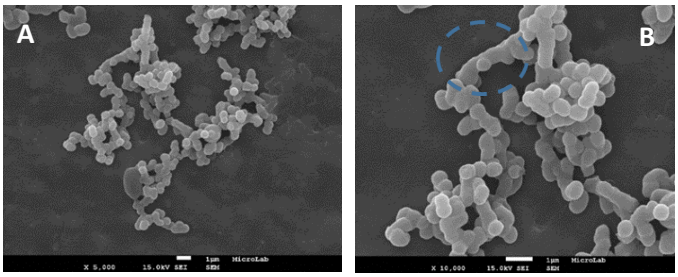

Figure 5. SEM micrograph of TiNPs induced by CBM3-R5 in 50 mM phosphate buffer at pH 7 (scale bar of 1 µm). Micrographs were obtained with magnifications of x 5, 000 (A) and x 10, 000 (B).

Precipitation of SiNPs on paper via CBM-R5 and R5

A set of experiments were performed to evaluate if the immobilized CBM-R5 and R5 were able to drive silica precipitation on paper. For this purpose, circular reaction areas (4 mm diameter) defined by a uniform hydrophobic barrier were firstly created on the paper being able to contain aqueous liquids within. Subsequently, certain amounts R5 or CBM3-R5 (1 µL) were added to each circular reaction area and allowed to dry for 30 minutes at room temperature. Three amounts of CBM-R5 and R5 were tested (3 000 pmol, 30 pmol and 3 pmol) and allowed to dry for 30 minutes at room temperature. Each circular reaction area was then individualized by cutting paper into 1 cm x 1 cm squares. Precipitation reactions were then performed by immersing each square piece of paper in 1 mL of a 91 mM solution of silicic acid in phosphate buffer at pH 7 for 5 minutes at room temperature. As control, paper pieces without protein were used, which were also immersed in silicic acid solution. After 5 minutes of incubation, samples were taken from the solutions and let to dry at room temperature. The analysis of the results in paper assays was a big challenge as the silica material is a white compound, which shares the same color as the paper. In fact, no differences in the aspect of the circular areas were observed by visual inspection. Thus, the analysis of precipitation on paper was highly dependent on SEM.

Clear differences in the results were detected when circular areas of paper prepared with 3 000 pmol of CBM3-R5 and R5 were observed at lower magnification by SEM. As it is possible to observe in Figure 6, which shows a composite image of areas prepared with R5 (left) and CBM3-R5 (right), formation of SiNPs revealed itself by the presence of a whitish material that contrasts strongly with the paper background. Furthermore, it is very clear that CBM3-R5 allows silica precipitation to occur over the entire surface of the paper circle (Figure 6, Left). Thus, a more uniform immobilization of R5 and hence of SiNPs was possible with the CBM3-R5 fusion because CBM3 contains binding sites involved in the recognition of the flat surface of crystalline cellulose (Tormo et al., 1996). Also, it seems that the R5 did not affected the ability of the CBM3 to bind to cellulose. When R5 was used alone, immobilization and silica precipitation on the cellulose surface were clearly more heterogeneous, with the peptide and silica predominating in the circle periphery. As expected, no silica particles were observed in the control experiments performed without protein.

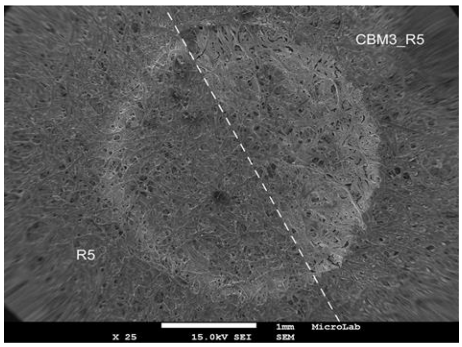

Figure 6. Composite image of SEM micrographs of circular areas of paper prepared with 3000 nmol of R5 (left) and CBM3-R5 (right), and after immersion on a 91 mM silicic acid solution for 5 min. The formation of silica over paper is apparent by the presence of a whitish material that contrasts strongly with the paper background. Scale bar of 1 mm.

SEM micrographs obtained at higher magnifications show that the morphology of the precipitated silica obtained with R5 and CBM3-R5 is very similar (Figure 7). The images show the presence of a densely packed network of fused and clustered silica particles laying over the network of cellulose fibers and fibrils characteristic of the paper matrix. The individual particles obtained with R5 (Figure 7) had an average size of about 213 ± 77 nm and individual particles obtained with CBM3-R5 (Figure 7) had an average size of about 231 ± 39 nm.

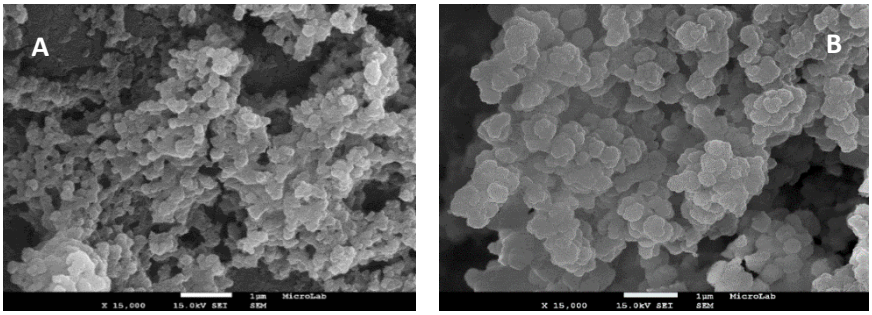

Figure 7. SEM micrographs of circular areas of paper prepared with 3000 pmol of R5 (left) and CBM3-R5 (right) after immersion on a 91 mM silicic acid solution for 5 min. Micrographs were obtained with magnification of x 15, 000 (A, B). Scale bar of 1 µm.

Attempts were also made to precipitate silica over paper using lower amounts of R5 and CBM3-R5 (30 and 3 pmol) in order to decrease particle density and eventually change morphology. However, precipitation was only observed with an amount of 3 pmol of R5 (Figure 8). As expected, the silica particles obtained in this case were more individualized and dispersed over the cellulose fibers and no formation of dense aggregates of silica were observed, as found with 3 000 pmol of R5 and CBM-R5. The mean diameter of the spherical SiNPs was 228 ± 42 nm. Thus, the remarkable difference between 3 pmol and 3000 pmol of peptide can be due the requirement of peptide self-assemble aggregates that appear to be required for silica precipitation (Knecht and Wright, 2003). No precipitation of SiNPs occurred over the cellulose fibers for 30 pmol either of R5 or CBM-R5. These results were not expected because the 3 pmol of R5 peptide was able to promote silica precipitation on the paper. Thus, it should be made more tests to overcome this problem.

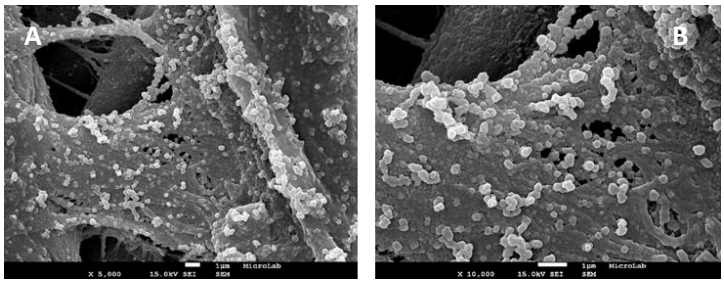

Figure 8. SEM micrographs of circular areas of paper prepared with 3 pmol of R5 after immersion on a 91 mM silicic acid solution for 5 min. A, B micrographs are presented with magnifications of x 5, 000, x 10, 000, respectively. Scale bar of 1 µm.

In contrast to what was observed for silica, the titanium dioxide nanoparticles were not detected over the cellulose fibers of paper by SEM analysis. This result was not expected because CBM3-R5 protein has shown titanium dioxide activity in the solution (Figure 24). Even though both conditions were the same for silica and titanium, the obtained results were not conclusive. Thus, more assays should be repeated in an attempt to overcome this problem.

Conclusions

As a first step towards this goal, the R5-induced precipitation of silica and titanium dioxide nanoparticles in solution was studied. Under the conditions studied (1.5 mM R5, 91 mM precursor, 50 mM phosphate buffer pH 7, 5 min), 71% and 50% of the silica and titanium dioxide precursors precipitated. The specific activity of R5 for silica and titanium dioxide precipitation was 8.64 ± 2.21 nmol Si/min.nmol R5 and 6.0

± 1.0 nmol Ti/ min.nmol R5, respectively. SEM analysis showed extensive agglomerates of fused nanoparticles in both cases. The ability of R5 and CBM-R5 to precipitate silica and titanium dioxide *in situ*, over cellulose fibers of chromatographic paper was investigated. When used at a density of 3 000 pmol/0.13 cm^2, both pre-immobilized R5 (via physical adsorption) and CBM3-R5 (by affinity interactions) were able to precipitate silica, yielding densely packed networks of fused and clustered particles over the cellulose fibers and fibrils in paper. Individual particles obtained with R5 and CBM3-R5 had an average size of around 213 ± 78 nm and 231 ± 39 nm, respectively. Precipitation of silica was not observed when lowering the amount of protein to 30 pmol and 3 pmol per 0.13 cm^2, with the exception of 3 pmol of R5. In this case, silica nanoparticles (228 ± 42 nm) were more individualized and dispersed over the cellulose fibers and no formation of dense aggregates of silica were observed.

In future experiments, intermediate protein amounts (e.g. 300 pmol per 0.13 cm^2) should be tested in order to evaluate the influence of the protein amount for silica precipitation on the cellulose fibers. Also, the precipitation reaction could be promoted by pipetting 1 µl or more of the precursor solution instead of immersing the paper in precursor solution, in order to better control the process. Another analyze that could be made is to determine the specific precipitation activity of CBM3-R5 in solution for both inorganic materials (silica and titanium dioxide).

Concerning future applications with silica/cellulose hybrid composite, it should me mentioned that, the surface of silica could be functionalized with linker molecules for example amine, thiol, among others in order to promote the attachment of biomolecule to the silica surface (Ali et al., 2014). This method can be used to design a based paper biosensor.

References

Abdullahil, K.; Maniruzzaman, M.; Kan, B.-W.; Kim, J. Fabrication and Characterization of Titanium Dioxide-Cellulose Composite and Its Urea Biosensing Behavior. **2015**, *27* (7), 539–548.

Ali, Y.; Zohre, R.; Mostafa, J.; Samaneh, R. Dye-Doped Fluorescent Nanoparticles in Molecular Imaging : A Review of Recent Advances and Future Opportunities. **2014**, *11* (2), 102–113.

Arfi, Y.; Shamshoum, M.; Rogachev, I.; Peleg, Y.; Bayer, E. A. Integration of Bacterial Lytic Polysaccharide Monooxygenases into Designer Cellulosomes Promotes Enhanced Cellulose Degradation. *Proc. Natl. Acad. Sci.* **2014**, *111* (25), 9109–9114.

Blake, A. W.; McCartney, L.; Flint, J. E.; Bolam, D. N.; Boraston, A. B.; Gilbert, H. J.; Knox, J. P. Understanding the Biological Rationale for the Diversity of Cellulose-Directed Carbohydrate-Binding Modules in Prokaryotic Enzymes. *J. Biol. Chem.* **2006**, *281* (39), 29321–29329.

Buzea, C.; Pacheco, I. I.; Robbie, K. Nanomaterials and Nanoparticles: Sources and Toxicity. *Biointerphases* **2007**, *2* (4), 17–71.

Choi, O.; Kim, B.-C.; An, J.-H.; Kyongseon, M.; Kim, Y. H.; Um, Y.; Oh, M.-K.; Sang, B.-I. A Biosensor Based on the Self-Entrapment of Glucose Oxidase within Biomimetic Silica Nanoparticles Induced by a Fusion Enzyme. *Ezyme Microb. Technol.* **2011**, *49* (5), 441–445.

Cole, K. E.; Ortiz, A. N.; Schoonen, M. A.; Valentine, A. M. Peptide- and Long-Chain Polyamine- Induced Synthesis of Micro- and Nanostructured Titanium Phosphate and Protein Encapsulation. *Chem. Mater.* **2006**, *18* (19), 4592–4599.

Coradin, T.; Eglin, D.; Livage, J. The Silicomolybdic Acid Spectrophotometric Method and Its Application to Silicate/biopolymer Interaction Studies. *Spectroscopy* **2004**, *18* (4), 567–576.

Emond, S.; Guieysse, D.; Lechevallier, S.; Dexpert-Ghys, J.; Monsan, P.; Remaud-Siméon, M. Alteration of Enzyme Activity and Enantioselectivity by Biomimetic Encapsulation in Silica Particles. *Chem. Commun.* **2012**, *48* (9), 1314–1316.

Gholami, T.; Salavati-Niasari, M.; Bazarganipour, M.; Noori, E. Synthesis and Characterization of Spherical Silica Nanoparticles by Modified Stöber Process Assisted by Organic Ligand. *Superlattices Microstruct.* **2013**, *61*, 33–41.

Grillo, R.; Rosa, A. H.; Fraceto, L. F. Engineered Nanoparticles and Organic Matter: A Review of the State-of-the-Art. *Chemosphere* **2015**, *119*, 608–619.

Knecht, M. R.; Wright, D. W. Functional Analysis of the Biomimetic Silica Precipitating Activity of the R5 Peptide from Cylindrotheca Fusiformis. *Chemical Communications*. 2003, pp 3038–3039.

Kröger, N.; Deutzmann, R.; Sumper, M. Polycationic Peptides from Diatom Biosilica That Direct Silica Nanosphere Formation. *Science (80-.).* **1999**, *286* (5442), 1129–1132.

Kröger, N.; Deutzmann, R.; Bergsdorf, C.; Sumper, M. Species-Specific Polyamines from Diatoms Control Silica Morphology. *Proc. Natl. Acad. Sci.* **2000**, *97* (26), 14133–14138.

Kröger, N.; Deutzmann, R.; Sumper, M. Silica-Precipitating Peptides from Diatoms: The Chemical Structure of Silaffin-1A from Cylindrotheca Fusiformis. *J. Biol. Chem.* **2001**, *276* (28), 26066–26070.

Kröger, N.; Lorenz, S.; Brunner, E.; Sumper, M. Self-Assembly of Highly Phosphorylated Silaffins and Their Function in Biosilica Morphogenesis. *Science (80-.).* **2002**, *298* (5593), 584–586.

Lechner, C. C.; Becker, C. F. W. A Sequence-Function Analysis of the Silica Precipitating Silaffin R5 Peptide. *J. Pept. Sci.* **2014**, *20* (2), 152–158.

Lechner, C.; Becker, C. Silaffins in Silica Biomineralization and Biomimetic Silica Precipitation. *Mar. Drugs* **2015**, *13* (8), 5297–5333.

Li, M.; Yin, J.-J.; Wamer, W. G.; Lo, Y. M. Mechanistic Characterization of Titanium Dioxide Nanoparticle-Induced Toxicity Using Electron Spin Resonance. *J. Food Drug Anal.* **2014**, *22* (1), 76–85.

Li, Z.; Percival, S. S.; Bonard, S.; Gu, L. Fabrication of Nanoparticles Using Partially Purified Pomegranate Ellagitannins and Gelatin and Their Apoptotic Effects. *Mol. Nutr. Food Res.* **2011**, *55* (7), 1096–1103.

Moharir, A.V., Sarma, K.A., Murti Krishna, R. S. R. Spectrophotometric Determination of Titanium with Tiron. **1972**, *17*, 167–172.

Naik, R. R.; Whitlock, P. W.; Rodriguez, F.; Brott, L. L.; Glawe, D. D.; Clarson, S. J.; Stone, M. O. Controlled Formation of Biosilica Structures in Vitro. *Chem. Commun.* **2003**, No. 2, 238–239.

Nam, D. H.; Won, K.; Kim, Y. H.; Sang, B. I. A Novel Route for Immobilization of Proteins to Silica Particles Incorporating Silaffin Domains. *Biotechnol. Prog.* **2009**, *25* (6), NA – NA.

Nelson, M. D.; Arrington, M. J. SOP for Analyzing Silicate (Microscale) by Using Manual Colorimetric Method. **2010**, 4–6.

Oliveira, C.; Carvalho, V.; Domingues, L.; Gama, F. M. Recombinant CBM-Fusion Technology — Applications Overview. *Biotechnol. Adv.* **2015**, *33* (3-4), 358–369.

Otzen, D. The Role of Proteins in Biosilicification. *Scientifica (Cairo).* **2012**, *2012*, 1–22.

Parkinson, J.; Gordon, R. Beyond Micromachining: The Potential of Diatoms. *Trends Biotechnol.* **1999**, *17* (5), 190–196.

Prathna, T. C.; Mathew, L.; Chandrasekaran, N.; Raichur, M. A.; Mukherjee, A. Biomimetic Synthesis of Nanoparticles: Science, Technology & Applicability. In *Biomimetics Learning from Nature*; Mukherjee, A., Ed.; InTech, 2010; pp 1–20.

Raman, N.; Sudharsan, S.; Pothiraj, K. Synthesis and Structural Reactivity of Inorganic–organic Hybrid Nanocomposites – A Review. *J. Saudi Chem. Soc.* **2012**, *16* (4), 339–352.

Rosa, A.; Louro, F.; Martins, S.; Inácio, J.; Azevedo, A.; Prazeres, M. Capture and Detection of DNA Hybrids on Paper via the Anchoring of Antibodies with Fusions of Carbohydrate Binding Modules and ZZ-Domains. *Anal. Chem.* **2014**, *86* (9), 4340–4347.

Senior, L.; Crump, M. P.; Williams, C.; Booth, P. J.; Mann, S.; Perriman, A. W.; Curnow, P. Structure and Function of the Silicifying Peptide R5. *J. Mater. Chem. B* **2015**, *3* (13), 2607–2614.

Sewell, S. L.; Wright, D. W. Biomimetic Synthesis of Titanium Dioxide Utilizing the R5 Peptide Derived from Cylindrotheca F Usiformis. *Chem. Mater.* **2006**, *18* (13), 3108–3113.

Smijs, T.; Pavel, S. Titanium Dioxide and Zinc Oxide Nanoparticles in Sunscreens: Focus on Their Safety and Effectiveness. *Nanotechnol. Sci. Appl.* **2011**, *4* (1), 95–112.

Sumper, M.; Kröger, N. Silica Formation in Diatoms: The Function of Long-Chain Polyamines and Silaffins. *J. Mater. Chem.* **2004**, *14* (14), 2059–2065.

Taha, A. A.; Wu, Y. na; Wang, H.; Li, F. Preparation and Application of Functionalized Cellulose Acetate/silica Composite Nanofibrous Membrane via Electrospinning for Cr(VI) Ion Removal from Aqueous Solution. *J. Environ. Manage.* **2012**, *112*, 10–16.

Tamba, B. I.; Dondas, A.; Leon, M.; Neagu, A. N.; Dodi, G.; Stefanescu, C.; Tijani, A. Silica Nanoparticles: Preparation, Characterization and in Vitro/in Vivo Biodistribution Studies. *Eur. J. Pharm. Sci.* **2015**, *71*, 46–55.

Thermo Fischer scientific Inc. INSTRUCTIONS BCA ™ Protein Assay Kit. *Publication Manual*. 2002, pp 1–7.

Tormo, J.; Lamed, R.; Chirino, a J.; Morag, E.; Bayer, E. a; Shoham, Y.; Steitz, T. a. Crystal Structure of a Bacterial Family-III Cellulose-Binding Domain: A General Mechanism for Attachment to Cellulose. *EMBO J.* **1996**, *15* (21), 5739–5751.

Yaniv, O.; Fichman, G.; Borovok, I.; Shoham, Y.; Bayer, E. A.; Lamed, R.; Shimon, L. J. W.; Frolow, F. Fine-Structural Variance of Family 3 Carbohydrate-Binding Modules as Extracellular Biomass-Sensing Components of Clostridium Thermocellum Anti-σ I Factors. *Acta Crystallogr. Sect. D Biol. Crystallogr.* **2014**, *70* (2), 522–534.